Attribution of the March 2021 exceptional dust storm in North China

Zhiyuan Hu, Yuanyuan Ma, Qinjian Jin,
Nkurunziza Fabien Idrissa, Jianping Huang,
and Wenjie Dong

AFFILIATIONS: Hu and Dong—School of Atmospheric Sciences, and Key Laboratory of Tropical Atmosphere-Ocean System, Ministry of Education, Sun Yat-sen University, and Southern Marine Science and Engineering Guangdong Laboratory Zhuhai, China; **Ma**—Key Laboratory of Land Surface Process and Climate Change in Cold and Arid Regions, Northwest Institute of Eco-Environment and Resources, Chinese Academy of Sciences, Lanzhou, and School of Atmospheric Sciences, and Key Laboratory of Tropical Atmosphere-Ocean System, Ministry of Education, Sun Yat-sen University, Zhuhai, China; **Jin**—Department of Geography and Atmospheric Science, University of Kansas, Lawrence, Kansas; **Idrissa**—School of Earth and Space Sciences, University of Science and Technology of China, Hefei, China; **Huang**—Collaborative Innovation Centre for West Ecological Safety, Lanzhou University, Lanzhou, China

CORRESPONDING AUTHOR: Jianping Huang, hjp@lzu.edu.cn

The post-1980 regional climate change increased dust AOD by +12.5 ± 15.0% and +43.6 ± 31.2% over the source and downstream areas respectively during a record-breaking dust storm in March 2021 in North China.

One unexpectedly strong mega sand and dust storm (SDS) swept north China during 14–18 March 2021, which was identified as one of the top 10 extreme weather and climate events of 2021 in China (Yin et al. 2022). This extreme SDS event greatly degraded the air quality over large areas of more than 3.8 million km², accounting for about 40% of China's land area, and affected 6.417 million people. For example, the surface particulate matter (PM_{10}) concentration exceeded the monitoring threshold in Ulanqab (~9,985 μg m^{-3}) and reached extraordinarily high values in Beijing (~7,400 μg m^{-3}) and Tianjin (~2,200 μg m^{-3}) along the transport pathway, far exceeding air quality standards (150 μg m^{-3}) and reaching extremely hazardous levels (Filonchyk 2021). In terms of intensity, persistence, and geographic range, this SDS event was an extremely rare weather event. As such, this event received extensive media exposure and was described as the biggest SDS in almost a decade by CNN (https://edition.cnn.com/2021/03/15/asia/beijing-sandstorm-decade-intl-hnk). A large number of buildings and crops were destroyed, resulting in direct economic losses of 30 million yuan (www.gov.cn/xinwen/2021-04-09/content_5598608.htm; ~4.5 million U.S. dollars).

In the context of climate change, the sea ice anomalies in the Barents and Kara Sea reversed from negative to positive during the winter of 2020/21, resulting in a sharp change in the cold air mass from the polar region. Consequently, this led to an increase in soil temperature and near-surface air temperature before this SDS event (Yin et al. 2022). Also, the warmest northwest Atlantic and coolest east Pacific (La Niña) during 2011/12–2020/21 jointly contributed to less precipitation in Mongolia, thus resulting in arid and dry soil conditions. These conditions were indirectly conducive to the occurrence of this strong SDS event under the influence of the super-strong Mongolian cyclone (Gui et al. 2022).

While the attribution of extreme events such as heat waves, drought, and extreme precipitation were routinely carried out (Du et al. 2020; Liu et al. 2022; Ma et al. 2022; Min et al. 2020; Zhou et al. 2018), there are few studies that focus on extreme SDS events. In this study, we for the first time applied high resolution simulations with a state-of-the-art regional chemical model and the "storyline" attribution approach (Ma et al. 2022; Shepherd et al. 2018) to quantify the contribution of climate change to this extreme SDS event.

Data and methods

Aerosol optical depth (AOD) defined as the column-integrated light extinction is a quantitative estimate of the amount of aerosol present in the atmosphere. The daily AOD at 550 nm retrieved from Visible Infrared Imaging Radiometer Suite (VIIRS) (Hsu et al. 2019) and Moderate Resolution Imaging Spectroradiometer (MODIS) aboard Terra and Aqua (Sayer et al. 2019) were used to examine this SDS event and to evaluate the model simulations. Also, the surface PM_{10} mass concentrations obtained from the China National Environmental Monitoring Center (CNEMC) network were used to describe the distribution characteristics of surface aerosol particles. The fifth generation of European Centre for Medium-Range Weather Forecasts atmospheric reanalysis data (ERA5) (Hersbach et al. 2020) was used to examine the atmospheric circulation (included geopotential height and wind field) and local meteorological (included surface temperature and precipitation) anomalies associated with this SDS event.

This SDS event occurred over the northwestern China (region 1, 36°–46°N, 90°–115°E) and greatly deteriorate air quality over the downstream areas (region 2, 36°–46°N, 115°–125°E) (Fig. 1a and Fig. ES1a). To quantify the magnitude of this event, the definition of an aerosol extreme event (AEE) was adopted from Pu and Jin (2021). In this study, an AEE was defined as a day or several consecutive days when the area-averaged (36°–46°N, 90°–115°E) daily AOD was above the 90th percentile of AOD centered on a 15-day window from March to May during 2003–21. The number of days within an AEE was its duration, and the averaged AOD within an AEE was its magnitude. Moreover, the maximum 1- and 5-day daily AOD in March–May from 2003 to 2021 were used to comprehensively examine the extreme characteristics of this event.

The impact of post-1980 regional climate change on this SDS event was investigated using the Weather Research and Forecasting Model coupled with a chemistry component (WRF-Chem) updated by the University of Science and Technology of China (Hu et al. 2016, 2019b; Zhao et al. 2014). The model was configured with 179 × 153 grid cells (10°–60°N, 55°–155°E) at 36 km × 36 km horizontal resolution and 40 vertical layers up to 50 hPa. The lateral boundary and initial meteorological conditions (LBCs) were obtained from the National Centers for Environmental Prediction final analysis data (https://rda.ucar.edu/datasets/ds083.2/). The related physics schemes followed Hu et al. (2019a, 2020), and the dust emission scheme was from Shao et al. (2011). To quantify regional climate change contributions, two seven-member ensemble experiments were performed: one with realistic LBCs (CTRL runs) versus the other with changed LBCs by removing the trend of the post-1980 regional climate change signals (DTREND runs) from the ERA5 data. The seven members were formed by
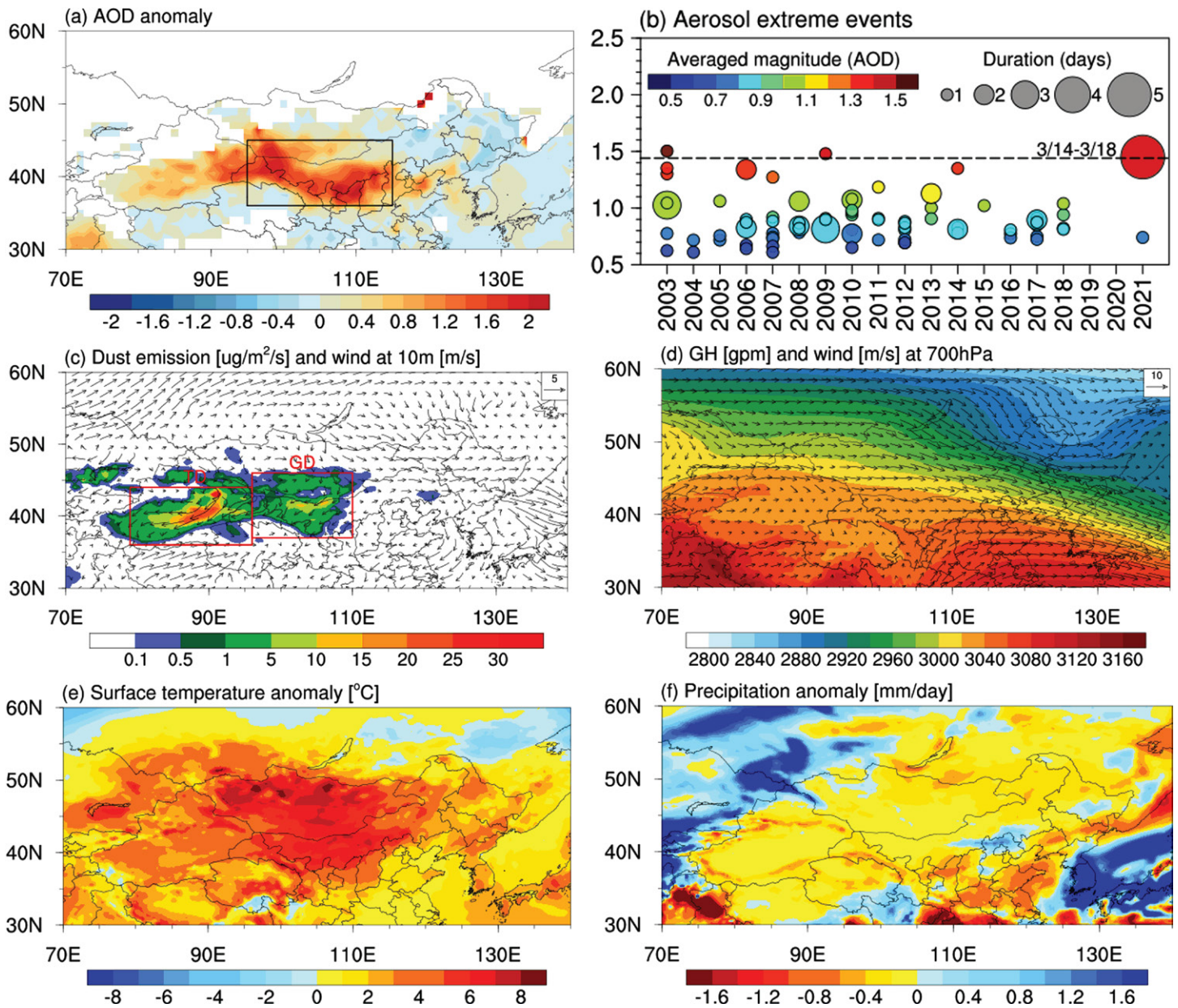
Fig. 1. (a) The observed MODIS AOD anomaly during 14–18 Mar 2021 related to all daily data from 14 to 18 Mar during 2003–21. The black box denoted the northwestern China (region 1: 36°–46°N, 90°–126°E). (b) Dust aerosol extreme events over East Asia. Magnitude (*y* axis) and duration (unit: day) of the extreme aerosol events over region 1 in March–May from 2003 to 2021. Size and color of the bubbles indicate the duration and averaged magnitude of the events, respectively. The dotted line is the magnitude of the averaged AOD during 14–18 Mar 2021. Data are from combined MODIS *Terra* and *Aqua*. (c) Dust emissions (shading) from MERRA-2 and wind vectors at 10 m from ERA5 during 14–18 Mar 2021. Red boxes are Taklimakan Desert and Gobi Desert. (d) The geopotential height (shading) and wind vectors at 700 hPa from ERA5. (e),(f) Anomalies of surface temperature and precipitation during 14–18 Mar 2021 related to 1981–2010 climatology from ERA5.

initializing the model using atmospheric conditions 6 h apart from 0000 UTC (coordinated universal time) 13 March 2021 to 0000 UTC 20 March 2021. The trend is estimated using the linear least squares following Ma et al. (2022) and Kawase et al. (2020), and the detrended variables include temperature, relative humidity, geopotential height, and horizontal winds at all pressure levels. Therefore, the impact of regional climate change on the SDS event was quantified as the difference between the ensemble average of all seven CTRL and DTREND runs.

Results

The magnitude of AOD anomaly during this SDS event was up to 2 over large parts of north China during 14–18 March 2021 (Fig. 1a), and these aerosol particles even propagated to the northern part of south China (Gui et al. 2022). As such, the monitoring PM_{10} from CNEMC reached more than 9,000 μg m^{-3} over the dust sources and 2,000–7,000 μg m^{-3} over the downstream areas, far exceeding air quality guidelines (45 μg m^{-3}) newly released by the World Health Organization and seriously threatening human health (Fig. ES1a in the online supplemental material). Over region 1, the areal average daily AOD was extremely high with a value of 1.4 during 14–18 March 2021. This extreme SDS event was ranked the first and third in terms of its duration and magnitude during the past 19 years, respectively (Fig. 1b). Furthermore, the area-averaged anomaly of daily AOD, the maximum 1- and 5-day AOD in March were ranked the first with the magnitude of 0.95, 0.68, and 0.38, respectively, indicating that this SDS event was the most extreme event during 2003–21 (Fig. ES1b). To further examine how extreme this event was at a longer time scale, the dust AOD anomalies from Modern-Era Retrospective Analysis for Research and Applications, version 2 (MERRA-2; Gelaro et al. 2017), were also analyzed (Fig. ES1c). The result showed that this dust extreme event was ranked third during the past 42 years, consistent with the results from MODIS shown in Fig. 1b.

During this massive dust plume, intense dust emissions were produced by an exceptionally strong Mongolian cyclone over the Gobi Desert (GD), then crossed southern Mongolia and Taklamakan Desert (TD) and affected north China (Fig. 1c and Fig. ES1d). Although the magnitude of dust emissions from the TD was larger than that from the GD, more dust particles from the TD were blown westward due to the prevailing surface easterly winds. In contrast, the dust particles from the GD were emitted into the atmosphere by a strong Mongolian cyclone, and then transported to north China by northwesterly winds (Fig. 1c). Subsequently, these dust particles were transported to downstream areas blown by westerly winds (Fig. 1d) and were further enhanced by mixing with local dust emissions during the eastward transport.

Dust emissions are generally controlled by land surface conditions, near-surface wind, and precipitation (Chen et al. 2018; Hu et al. 2020; Huang et al. 2014; Pu and Jin 2021). During this event, the surface temperature showed a positive anomaly (more than 6°C) over the Mongolia and western Inner Mongolia (region 1, Fig. 1e) compared to climatology, while the precipitation presented a negative anomaly (less than −0.23 mm day^{-1}) of 2 weeks before this event (Fig. 1f). This indicated that these dust sources became drier and more easily eroded. Meanwhile, this high temperature anomaly favors the formation of a warm low pressure system near the ground (Gui et al. 2022), while the Mongolian cyclone became lower, which was conducive to aggravating gales through increasing the pressure gradient between the cold and high pressure. This suggests that the synoptic disturbances played an important role in the formation and transport of this extreme SDS event.

Ensemble simulations of the WRF-Chem model reproduced well the spatial distribution of AOD with a spatial correlation coefficient of 0.72 (Figs. 2a,b) over the whole simulated region (30°–60°N, 70°–140°E). Moreover, the surface PM_{10} mass concentrations from WRF-Chem were consistent with CNEMC observations with a correlation coefficient of 0.67 (Fig. ES1e). Overall, the model well captures the spatiotemporal characteristics of the SDS event that enabled a reliable attribution analysis.

The difference of dust AOD between the ensemble means of CTRL runs and DTREND runs showed that the regional climate change after 1980 significantly increased dust AOD over large parts of north China with a maximum value of 0.8 (Fig. 2c). The dust AOD increased by +0.15 ± 0.15 on average over region 1, with an increase of +12.5% ± 15.0% with respect to the mean dust AOD in the DTREND runs (Fig. 2d). Also, an increase of the dust AOD due to
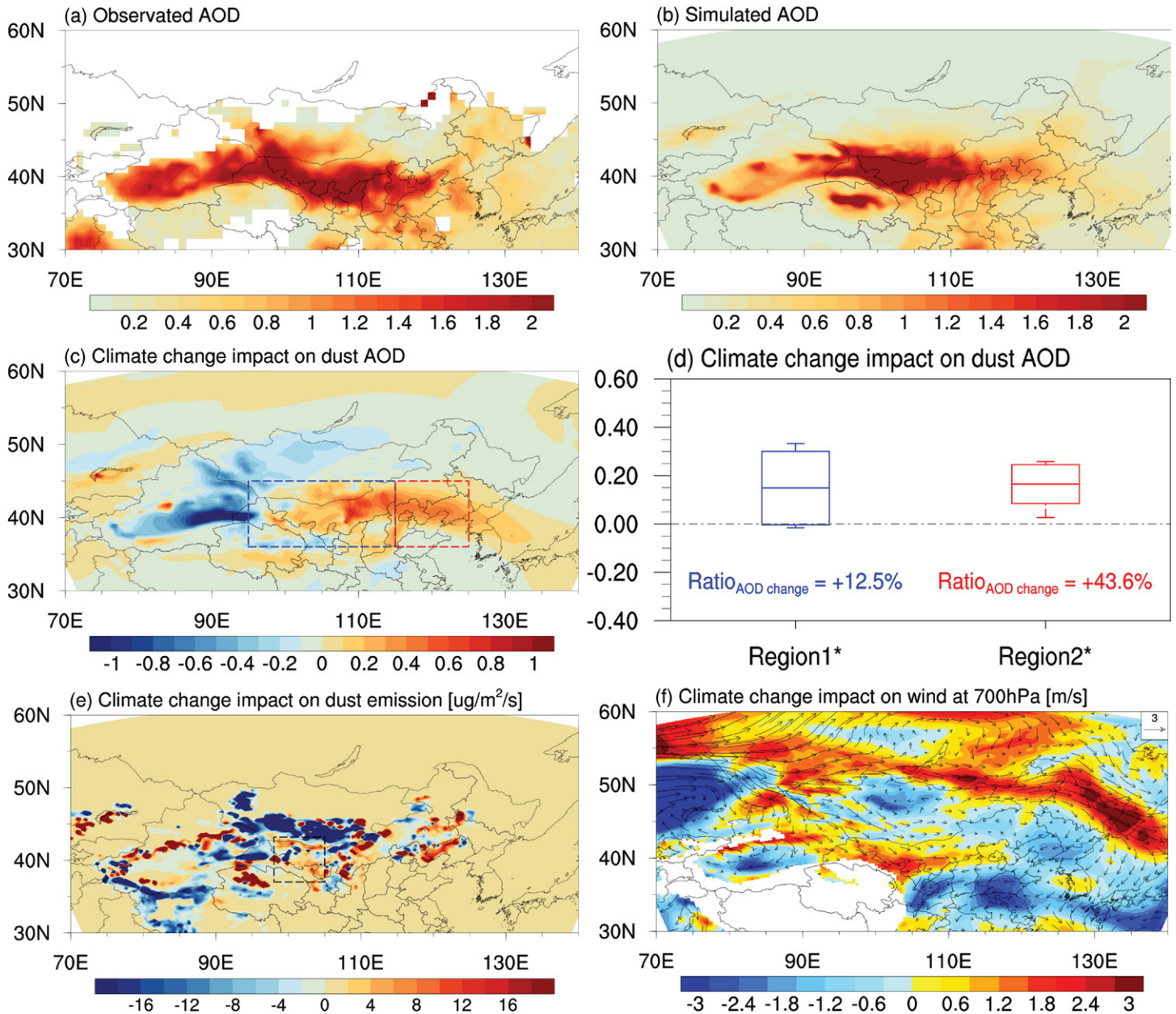
Fig. 2. (a) The observed AOD from MODIS and VIIRS retrievals during 14–18 Mar 2021. (b) As in (a), but from WRF-Chem CTRL simulations. (c) The climate change impact on dust AOD from the ensemble mean difference between the CTRL and DTREND runs during this dust event. Region 1 was the dust source region (blue box) and region 2 was the dust downstream areas (red box, 36°–46°N, 115°–125°E). (d) The area-averaged dust AOD induced by the climate change impact over region 1 and region 2 during this dust event. The line in the box and width of the box respectively represents the averaged value and standard deviations, and the whiskers show the minimum and maximum values. The ratio is the change percent of areal average of dust AOD as the regional climate change impact and is calculated as the percent of difference between Ensemble-mean$_{CTRL}$ vs Ensemble-mean$_{DTREND}$. The labels marked with "*" indicate a statistically significant difference between CTRL runs and DTREND runs at 90% confidence interval of t-test. (e),(f) The climate change impact on dust emission and wind field at 700 hPa from the ensemble mean difference between the CTRL and DTREND runs during this dust event.

regional climate change appeared over region 2 (red box in Fig. 2c) with the area-averaged value of +0.17 ± 0.08 corresponding to a percent of +43.6% ± 31.2% (Fig. 2d).

To explain the increase in dust AOD induced by regional climate change, we analyzed the dust emissions and atmospheric circulation. Typically, dust emissions over southern Mongolia and western Inner Mongolia increased in this extreme SDS event (Fig. 2e), which was directly associated with the increased surface wind speed over dust source region (Fig. ES1f) and

increased surface temperature (Fig. ES1g). Specifically, compared with the DTREND runs, the regional climate change increased the surface temperature by +2.6° ± 0.9°C, decreased the precipitation by 0.05 ± 0.15 mm day^{-1}, and strengthened the westerly wind speeds at 700 hPa by −0.07 ± 0.05 m s^{-1}, especially along the dust plume transport path (Fig. 2f). Overall, the regional climate changes in surface temperature, wind speed, and precipitation favored the dust emissions from the GD and their eastward transport.

Conclusions

The contribution of climate change to the exceptionally strong SDS during 14–18 March 2021 was quantitatively evaluated using a regional chemical model (WRF-Chem) based on a "storyline" approach. Compared with satellite retrievals, the WRF-Chem model simulations represented well AOD distribution characteristics over north China. Also, simulated surface PM$_{10}$ mass concentrations were consistent with ground observations. Sensitivity ensemble experiments, in which the post-1980 regional climate change signals were removed, showed that the dust AOD was increased due to climate change. The area-averaged dust AOD over the study areas including the downstream areas was respectively increased by +0.15 ± 0.15 and +0.17 ± 0.08, which is about +12.5% ± 15.0% and +43.6% ± 31.2% larger than that in the ensemble-mean of DTREND runs. These increases in dust AOD were induced by the influence of climate change on dust emissions over southern Mongolia and western Inner Mongolia and the atmospheric circulation, which was related to the increased surface temperature and wind speed. In conclusion, our results indicate that the post-1980 regional climate change significantly contributes to the strengthening of the March 2021 exceptional dust storm in north China. Note that some other contributing factors such as changes in land use are not included in this analysis. Our future work will address these factors to comprehensively explore the influence of the regional climate change on the occurrence probability of this dust extreme event.

References

Chen, S., and Coauthors, 2018: Quantifying contributions of natural and anthropogenic dust emission from different climatic regions. *Atmos. Environ.*, **191**, 94–104, https://doi.org/10.1016/j.atmosenv.2018.07.043.

Du, J., K. Wang, B. Cui, S. Jiang, and G. Wu, 2020: Attribution of the record-breaking consecutive dry days in winter 2017/18 in Beijing [in "Explaining Extreme Events of 2018 from a Climate Perspective"]. *Bull. Amer. Meteor. Soc.*, **101** (1), S95–S102, https://doi.org/10.1175/BAMS-D-19-0139.1.

Filonchyk, M., 2021: Characteristics of the severe March 2021 Gobi Desert dust storm and its impact on air pollution in China. *Chemosphere*, **287**, 132219, https://doi.org/10.1016/j.chemosphere.2021.132219.

Gelaro, R., and Coauthors, 2017: The Modern-Era Retrospective Analysis for Research and Applications, version 2 (MERRA-2). *J. Climate*, **30**, 5419–5454, https://doi.org/10.1175/JCLI-D-16-0758.1.

Gui, K., and Coauthors, 2022: Record-breaking dust loading during two mega dust storm events over northern China in March 2021: Aerosol optical and radiative properties and meteorological drivers. *Atmos. Chem. Phys.*, **22**, 7905–7932, https://doi.org/10.5194/acp-22-7905-2022.

Hersbach, H., and Coauthors, 2020: The ERA5 global reanalysis. *Quart. J. Roy. Meteor. Soc.*, **146**, 1999–2049, https://doi.org/10.1002/qj.3803.

Hsu, N. C., J. Lee, A. M. Sayer, W. Kim, C. Bettenhausen, and S. C. Tsay, 2019: VIIRS deep blue aerosol products over land: Extending the EOS long-term aerosol data records. *J. Geophys. Res. Atmos.*, **124**, 4026–4053, https://doi.org/10.1029/2018JD029688.

Hu, Z., C. Zhao, J. Huang, L. R. Leung, Y. Qian, H. Yu, L. Huang, and O. V. Kalashnikova, 2016: Trans-Pacific transport and evolution of aerosols: Evaluation of quasi-global WRF-Chem simulation with multiple observations. *Geosci. Model Dev.*, **9**, 1725–1746, https://doi.org/10.5194/gmd-9-1725-2016.

Hu, Z., and Coauthors, 2019a: Modeling the contributions of Northern Hemisphere dust sources to dust outflow from East Asia. *Atmos. Environ.*, **202**, 234–243, https://doi.org/10.1016/j.atmosenv.2019.01.022.

Hu, Z., and Coauthors, 2019b: Trans-Pacific transport and evolution of aerosols: Spatiotemporal characteristics and source contributions. *Atmos. Chem. Phys.*, **19**, 12 709–12 730, https://doi.org/10.5194/acp-19-12709-2019.

Hu, Z., J. Huang, Z. Zhao, Q. Jin, Y. Ma, and B. Yang, 2020: Modeling dust sources, transport, and radiative effects at different altitudes over the Tibetan Plateau. *Atmos. Chem. Phys.*, **20**, 1507–1529, https://doi.org/10.5194/acp-20-1507-2020.

Huang, J., T. Wang, W. Wang, Z. Li, and H. Yan, 2014: Climate effects of dust aerosols over East Asian arid and semiarid regions. *J. Geophys. Res. Atmos.*, **119**, 11 398–11 416, https://doi.org/10.1002/2014JD021796.

Kawase, H., Y. Imada, H. Tsuguti, T. Nakaegawa, and I. Takayabu, 2020: The heavy rain event of July 2018 in Japan enhanced by historical warming [in "Explaining Extreme Events of 2018 from a Climate Perspective"]. *Bull. Amer. Meteor. Soc.*, **101** (1), S109–S114, https://doi.org/10.1175/BAMS-D-19-0173.1.

Liu, F., B. Wang, Y. Ouyang, H. Wang, S. Qiao, G. Chen, and W. Dong, 2022: Intraseasonal variability of global land monsoon precipitation and its recent trend. *npj Climate Atmos. Sci.*, **5**, 30, https://doi.org/10.1038/s41612-022-00253-7.

Ma, Y., Z. Hu, X. Meng, F. Liu, and W. Dong, 2022: Was the record-breaking mei-yu of 2020 enhanced by regional climate change? *Bull. Amer. Meteor. Soc.*, **103**, S76–S82, https://doi.org/10.1175/BAMS-D-21-0187.1.

Min, S., Y. Kim, S. Lee, S. Sparrow, S. Li, F. C. Lott, and P. Stott, 2020: Quantifying human impact on the 2018 summer longest heat wave in South Korea [in "Explaining Extreme Events of 2018 from a Climate Perspective"]. *Bull. Amer. Meteor. Soc.*, **101** (1), S103–S108, https://doi.org/10.1175/BAMS-D-19-0151.1.

Pu, B., and Q. Jin, 2021: A record-breaking trans-Atlantic African dust plume associated with atmospheric circulation extremes in June 2020. *Bull. Amer. Meteor. Soc.*, **102**, E1340–E1356, https://doi.org/10.1175/BAMS-D-21-0014.1.

Sayer, A. M., N. C. Hsu, J. Lee, W. V. Kim, and S. T. Dutcher, 2019: Validation, stability, and consistency of MODIS collection 6.1 and VIIRS version 1 deep blue aerosol data over land. *J. Geophys. Res. Atmos.*, **124**, 4658–4688, https://doi.org/10.1029/2018JD029598.

Shao, Y., M. Ishizuka, M. Mikami, and J. F. Leys, 2011: Parameterization of size-resolved dust emission and validation with measurements. *J. Geophys. Res.*, **116**, D08203, https://doi.org/10.1029/2010JD014527.

Shepherd, T. G., and Coauthors, 2018: Storylines: An alternative approach to representing uncertainty in physical aspects of climate change. *Climatic Change*, **151**, 555–571, https://doi.org/10.1007/s10584-018-2317-9.

Yin, Z., Y. Wan, Y. Zhang, and H. Wang, 2022: Why super sandstorm 2021 in North China? *Natl. Sci. Rev.*, **9**, nwab165, https://doi.org/10.1093/nsr/nwab165.

Zhao, C., and Coauthors, 2014: Simulating black carbon and dust and their radiative forcing in seasonal snow: A case study over North China with field campaign measurements. *Atmos. Chem. Phys.*, **14**, 11 475–11 491, https://doi.org/10.5194/acp-14-11475-2014.

Zhou, C., K. Wang, and D. Qi, 2018: Attribution of the July 2016 extreme precipitation event over China's Wuhan [in "Explaining Extreme Events of 2016 from a Climate Perspective"]. *Bull. Amer. Meteor. Soc.*, **99** (1), S107–S112, https://doi.org/10.1175/BAMS-D-17-0090.1.